International Journal of Biological Macromolecules 91 (2016) 416–425

Contents lists available at ScienceDirect

International Journal of Biological Macromolecules

journal homepage: www.elsevier.com/locate/ijbiomac

Site-directed mutagenesis of a conserved Asn450 residue of *Bacillus licheniformis* γ-glutamyltranspeptidase

Min-Guan Lin[a,1], Meng-Chun Chi[b,1], Yu-Yi Chen[b], Tzu-Fan Wang[c], Hui-Fen Lo[d,*], Long-Liu Lin[b,*]

[a] *Institute of Molecular Biology, Academia Sinica, Nangang District, Taipei City 11529, Taiwan*
[b] *Department of Applied Chemistry, National Chiayi University, 300 Syuefu Road, Chiayi City 60004, Taiwan*
[c] *Department of Chemistry, National Cheng Kung University, Tainan City 701, Taiwan*
[d] *Department of Food Science and Technology, Hungkuang University, 1018 Taiwan Boulevard, Shalu District, Taichung City 43302, Taiwan*

ARTICLE INFO

Article history:
Received 3 February 2016
Received in revised form 27 May 2016
Accepted 28 May 2016
Available online 28 May 2016

Keywords:
γ-Glutamyltranspeptidase
Asparagine
Site-directed mutagenesis

ABSTRACT

Bacillus licheniformis γ-glutamyltranspeptidase (*Bl*GGT) belongs to N-terminal nucleophile hydrolase superfamily in which all inclusive members are synthetized as single-chain precursors, and then self-processed to form mature enzymes. Here we investigated the role of a conserved Asn450 residue in *Bl*GGT through site-directed mutagenesis and molecular characterization of four relevant variants. Substitution of Asn450 by arginine resulted in a significant reduction in the catalytic activity of *Bl*GGT. Conversely, N450A and N450D displayed an enhanced activity. The catalytic efficiency of *Bl*GGT was calculated to be 16.04 mM^{-1} s^{-1}, but this value was either decreased to 8.93 mM^{-1} s^{-1} in N450 K or increased to more than 123.65 mM^{-1} s^{-1} in N450A and N450D. In addition, the ratio of transpeptidation to hydrolysis was increased from 3.5 to more than 7.6 by the mutations. Structural analyses showed that fluorescence, circular dichroism spectra and thermal denaturation profiles of mutant proteins were essentially consistent with those of *Bl*GGT. However, guanidine hydrochloride (GdnHCl)-induced transition was significantly reduced in comparison with the wild-type enzyme. Molecular modeling suggests that residue Asn450 of *Bl*GGT is important to create suitable environments for both autoprocessing and catalytic reactions.

1. Introduction

γ-Glutamyltranspeptidase (GGT; EC 2.3.2.2) catalyzes the hydrolysis of linkage bonds in γ-glutamyl peptides and the subsequent transfer of the γ-glutamyl moiety to amino acids, peptides, or water [1]. This enzyme is widely distributed among living organisms [1,2], and plays a primary role in the metabolism of extracellular reduced glutathione (GSH), allowing for precursor amino acids to be assimilated and reutilized for the synthesis of intracellular GSH [3–5]. A number of reviews have further indicated that GGT is involved in many crucial cellular activities, such as aging, apoptosis and drug detoxification [6–8]. In humans, it links to several physiological disorders associated with oxidative stresses [9,10] and therefore is the commonly used marker for liver diseases [11], cardiovascular diseases [12], and cancer [13–16]. Besides its physiological function, GGT can be employed for the biocatalytic synthesis of various γ-glutamyl compounds with great potential to accelerate progress towards pharmaceutical and biotechnological applications [17–19].

So far, the enzymatic reaction of mature GGTs has been proposed to follow a classical ping-pong mechanism [18,20–22]. In the first step of the catalytic cycle, the γ-glutamyl moiety of the donor substrate reacts with the hydroxyl group of a conserved Thr in the active site to form a tetrahedral intermediate [18,20,22]. Subsequent release of the free amine donor from the intermediate leads to the generation of a covalent γ-glutamyl enzyme intermediate. The catalytic cycle is eventually completed by the transfer of γ-glutamyl moiety to an acceptor substrate, such as water (hydrolysis) or a dipeptide (transpeptidation). Although the role of transpeptidation in bacteria remains unclear [18,23], both hydrolysis and transpeptidation reactions are believed to be closely related to the physiological processes vital for a living organism.

The heterodimeric eukaryotic GGTs are frequently localized at the plasma membrane with their active site oriented to the extracellular space [24]; however, bacterial enzymes are present either in the cytosol or in the periplasmic space [4,18] and can

* Corresponding authors.
E-mail addresses: hflo@sunrise.hk.edu.tw (H.-F. Lo), llin@mail.ncyu.edu.tw (L.-L. Lin).
[1] These authors contributed equally to this work.

http://dx.doi.org/10.1016/j.ijbiomac.2016.05.101
0141-8130/

be heterodimeric [25–28] or heterotetrameric [23]. It has been demonstrated that the precursor proteins from both eukaryotic and prokaryotic organisms undergo the post-translational autoproteolytic processing to produce mature enzymes composed of a large (L) subunit and a small (S) subunit [20,29,30]. Experimental evidence has suggested that the N-terminal Thr of the S-subunit plays a key role in the autocatalytic processing of GGT enzymes. In the case of *Escherichia coli* GGT (*Ec*GGT), substitution of Thr391 by Ala hampers the maturation process of the enzyme, leading to the expression of a precursor-like protein that is unable to process itself [31]. This phenomenon has been consistently observed in other GGT enzymes, including *Bacillus licheniformis* GGT (*Bl*GGT) [32] and *Geobacillus thermodenitrificans* GGT (*Gt*GGT) [25]. Although the N-terminal truncation of *Bacillus pumilus* GGT (*Bp*GGT) seems not affect the maturation process [28], some other regions or residues can be responsible for the maturation process of GGT enzymes. With the help of gene deletion and site-specific mutagenesis techniques, our previous studies have shown that the selective removal of C-terminal residues of *Bl*GGT definitely cripples its autoprocessing to a heterodimer [33] and several other residues in the enzyme have also been demonstrated to be critical for the maturation process [32,34,35].

Based on the structural information of an *Ec*GGT mutant (T391A), a mechanism for the autoprocessing reaction of GGT enzymes has been proposed [36]. In this mechanism, a water molecule acts as an activator that is located at a proper position through intramolecular hydrogen bonds formed by the carbonyl oxygen of Ser388 and NH amide of Gly484 [36]. The presence of solvent molecules is considered to be of great important for the autoprocessing reaction of Ntn hydrolase superfamily [37]. Nevertheless, the involvement of solvent molecules in the autocatalytic processing of GGT is not universally accepted. Indeed, two polypeptide chains are present in the asymmetric unit of the X-ray structure of T391A-*Ec*GGT and a water molecule is located in the right position to act as activator only in one of the chains [36]. Furthermore, significant structural differences have been found between the mature *Ec*GGT and other bacterial and human counterparts [38]. A recent investigation by X-ray diffraction has indicated that *Bl*GGT contains a more opened active site cleft, which is not covered by a lid loop [39]. This structural feature is shared by human GGT [38], *Bs*GGT [40], and probably also by other bacterial counterparts [23,25,28]. Besides, some GGT enzymes, including *Bs*GGT, *Bp*GGT and *Bl*GGT, possess an extra sequence at the C-terminal end of the L-subunit (residues 384–398 in *Bl*GGT) [35]. This extra sequence has been reported to be important for the autocatalytic processing of the *Bl*GGT enzyme [35]. It is only very recently that basic aspects of the autocatalytic processing of GGT precursors have been established according to the crystal structure of a precursor mimic of *B. licheniformis* enzyme and mutagenesis studies [41]. In this study, we substituted the conserved asparagine 450 of *Bl*GGT with other amino acids in order to gain insights into the role of this residue. Mutations of Asn450 have been found to influence both autocatalytic processing and transpeptidase activity of *Bl*GGT, indicating the importance of this residue in the maturation of enzyme precursor and in the catalytic function.

2. Materials and methods

2.1. Reagents and bacterial strains

Two basic ingredients, bacto-tryptone and yeast extract, of Luria-Bertani (LB) medium were acquired from Difco Laboratories Inc. (Detroit, MI, USA). Gene-specific primers were synthesized by Mission Biotechnology Inc. (Taipei, Taiwan) and listed in Table 1. The QuikChange site-directed mutagenesis kit was brought from Stratagene (La Jolla, CA, USA). Nickel-nitrilotriacetic acid affinity resin was purchased from Qiagen Inc. (Valencia, CA, USA). L-γ-Glutamyl-*p*-nitroanilide (L-γ-Glu-*p*-NA), *p*-nitroaniline (*p*-NA) and Gly-Gly were obtained from Sigma-Aldrich Fine Chemicals (St. Louis, MO, USA). Reagents for polyacrylamide gel electrophoresis (PAGE) and protein concentration assay were acquired from Bio-Rad Laboratories (Hercules, CA, USA). All other chemicals were of commercially available and were used without further purification.

Table 1
Overlapping complementary primers used in the site-directed mutagenesis.

Protein	Nucleotide sequence (5′→3′)[a]	Codon change
N450Q	(f)-CCAGGCGGCGCCCAGGAAGTGCAGCCG (r)-CGGCTGCACTTC<u>CTG</u>GGCGCCGCCTGG	AAC → CAG
N450A	(f)-CCAGGCGGCGCC<u>GCG</u>GAAGTGCAGCCG (r)-CGGCTGCACTTC<u>CGC</u>GGCGCCGCCTGG	AAC → GCG
N450D	(f)-CCAGGCGGCGCC<u>GAC</u>GAAGTGCAGCCG (r)-CGGCTGCACTTC<u>GTC</u>GGCGCCGCCTGG	AAC → GAC
N450K	(f)-CCAGGCGGCGCC<u>AAA</u>GAAGTGCAGCCG (r)-CGGCTGCACTTC<u>TTT</u>GGCGCCGCCTGG	AAC → AAA

[a] The altered codons were underlined.

Escherichia coli Nova Blue (Novagen Inc., Madison, WI, USA) was employed in the maintenance of plasmids, whereas another *E. coli* strain (XL1-Blue; Stratagene, La Jolla, CA, USA) was used as a host for the construction of site-specific mutations. T5 RNA-polymerase-mediated gene expression was performed in *E. coli* M15 (pRep4) (Qiagen). All strains of *E. coli* were grown aerobically in LB medium at either 28 °C or 37 °C. As required, antibiotics ampicillin and kanamycin were added to the medium at a final concentration of 100 μg/mL and 25 μg/mL, respectively.

2.2. Multiple sequence alignment and computer modeling

The amino acid sequence of *Bl*GGT was aligned with the counterpart sequences from various other species using Clustal program [42]. The Swiss-Prot accession codes for the GGT enzymes were as follows: *Bl*GGT (Q62WE3), *Bp*GGT (F8SVM6), *Bs*GGT (P54422), *Bacillus amyloliquefaciens* GGT (*Ba*GGT; E1UV41), *Thiobacillus denitrificans* GGT (*Td*GGT; Q3SJ07), *Ec*GGT (P18956), *Labrenzia aggregata* GGT (*La*GGT; A0NWX8), *Helicobacter pylori* GGT (*Hp*GGT; O25743), *Pseudomonas aeruginosa* GGT (*Pa*GGT; Q9I406), and *Gt*GGT (A4ITG5).

Molecular models of mutant enzymes were established at SWISS MODEL Server [43] with the X-ray crystal structures of *Bl*GGT (PDB code: 4OTT) and T399A-*Bl*GGT (PDB code: 4Y23) as the templates. The models were further improved by iterative cycles of manual fitting using Coot [44] and refinement by Phenix [45].

2.3. Site-directed mutagenesis

A previous constructed plasmid pQE-*Bl*GGT [26] was used as the template for PCR-based site-directed mutagenesis. The reaction mixture (50 μL) consisted of 10 ng of template DNA, 0.2 μM of forward and reverse primers, 0.2 mM of dNTP, and 2.5 U of high fidelity *PfuTurbo* DNA polymerase. Following 16 runs of the thermal cycling program (95 °C for 30 s, 58 °C for 1 min, and 68 °C for 10 min), the PCR products were treated with *Dpn*I endonuclease that digests the hemimethylated template leaving behind the nicked DNA with the mutation of interest. Thereafter, the digested product was transformed into *E. coli* XL-1 Blue supercompetent cells, and single colonies were picked up from the LB plates by a sterilized loop for the verification of mutations by DNA sequencing.

2.4. Expression and purification of wild-type and mutant enzymes

E. coli M15 (pRep4) cells harboring either pQE-*Bl*GGT or each of the mutated plasmids were grown in 100 mL of LB broth supplemented with antibiotics at 37 °C. Until the OD_{600} reached 0.8–1.0, isopropyl-β-D-thiogalactopyranoside (IPTG) was added to the broth at a final concentration of 0.1 mM and the culture was continually incubated at 28 °C for an additional 6 h. The cells were then harvested by centrifugation at 12,000*g* for 20 min and washed twice with 50 mL of Tris-HCl buffer (25 mM, pH 9.0). Purification of wild-type and mutant enzymes was performed as described previously [32]. Protein purity and the degree of autocatalytic processing were checked by SDS – PAGE using the Laemmli buffer system [46]. The degree of autocatalytic processing was evaluated by quantifying the intensity of protein bands in the gels with a computerized densitometer using CP ATCAS 2.0 program (http://www.lazarsoftware.com). Protein concentrations were determined with the Bio-Rad protein assay reagent using bovine serum albumin as a concentration standard.

2.5. Activity assay and enzyme kinetics

The enzymatic activity of *Bl*GGT and its variants was measured by a discontinuous colorimeter assay as described previously [47]. Briefly, each enzyme and the reaction components (1.25 mM L-γ-Glu-*p*-NA, 30 mM Gly-Gly, 1 mM $MgCl_2$, and 50 mM Tris-HCl buffer; pH 9.0) were incubated separately at 40 °C for 10 min. The reaction was initiated by adding 20-μL enzyme solution at a suitable dilution and enough distilled water to bring the final volume to 1 mL. After incubating the mixture at 40 °C for 10 min, the reaction was quenched by the addition of 100 μL acetic acid (3.5 N). The amount of *p*-NA in the reaction solution was determined by monitoring the absorbance changes at 410 nm using a UV–vis spectrophotometer. One unit of GGT activity is defined as the amount of enzymes that produce 1 μmol of *p*-NA per minute under the assay conditions.

The K_M and k_{cat} values of wild-type and mutant enzymes were estimated by measuring *p*-NA formation in 1 mL reaction mixtures with various concentrations of L-γ-Glu-*p*-NA (0.1–2.0 K_M) and a fixed concentration (30 mM) of dipeptide acceptor Gly-Gly in 50 mM Tris-HCl buffer (pH 9.0). To estimate the kinetic constants, a Lineweaver—Burk plot was created with data points derived from double-reciprocal transformation. All kinetic experiments were performed at least three times.

2.6. Circular dichroism (CD) and fluorescence studies

CD spectra were recorded by a jasco-815 spectrophotopolarimeter (JASCO, Japan) equipped with a Peltier thermostatic system under constant nitrogen flux at room temperature and with a 0.1-cm quartz cuvette. Each spectrum represented the average of three accumulations recorded between wavelengths of 200 and 250 nm, with a resolution of 0.2 nm, a bandwidth of 0.5 nm, a response time of 4 s, a sensitivity of 100 mdeg, and a scan speed of 20 nm/min. All spectra were corrected for background by the subtraction of the buffer blank. The molar residue ellipticity (θ) was calculated using the formula: $[\theta] = \theta_{obs}$ (in mdeg)/(molar concentration of the protein × path length (in nm) × number of amino acid residues in the protein) [48]. The CD intensity was reported in molar residue ellipticity (MRE) with the units of deg cm^2 $dmol^{-1}$.

Steady-state emission spectra were recorded with a jasco FP-6500 spectrofluorometer at an excitation wavelength of 280 nm using a 0.5-mL quartz cuvette. The emission spectra of protein samples with a concentration of approximately 14.5 μM were measured from 300 to 400 nm under the scanning speed of 240 nm/min. The contribution of buffer components to the fluorescence was subtracted from all the spectra. Each spectrum was obtained in triplicate with virtually identical results.

3. Results and discussion

3.1. Multiple sequence alignment and the local environment of Asn450

Consistent with other GGT structures determined so far, *Bl*GGT adopts the conserved fold of proteins belonging to the Ntn hydrolase family [37]. In the crystal structure of *Bl*GGT [39], the large subunit contains a globular domain consisting of 14 α-helices, six small 3_{10} helices and 11 β-strands, and the small subunit comprises of 3 α-helices, two small 3_{10} helices and 11 β-strands. Furthermore, both subunits provide strands to a nearly flat β-sheet that constitutes the core of the heterodimeric arrangement. Unlike their structural consistency, the primary structure of GGT enzymes displays a great degree of variability. The small subunit spanning the *Bl*GGT residues 399–585 only exhibits a sequence identity of 33–78% with *Bacillus subtilis*, *E. coli*, *H. pylori*, *Pseudomonas aeruginosa* counterparts, and identities with the corresponding subunit of non-microbial enzymes (such as bovine, human, and mouse GGTs) are ranged from 25 to 31%. The results of multiple sequence alignment show that an asparagine residue (equivalent to Asn450 of *Bl*GGT) located on the small subunit of microbial GGT enzymes is strictly conserved (Fig. 1). Although the involvement of a conserved threonine residue in the autocatalytic processing of GGT enzymes has been extensively studied [23,29,32,49], there is still no report dealing with the importance of this Asn residue on the maturation process of the *Bl*GGT precursor. With current progress in the structural determination of GGT enzymes, the crystal structures of the precursor mimic of *Ec*GGT and *Bl*GGT attributes new insight into the maturation mechanism of this type of proteins [36,41]. Structural data of the precursor mimic of *Bl*GGT suggest that Thr417 is situated at a competent position to activate the catalytic threonine (Thr399) for subsequent nucleophilic attack of the scissile peptide bond, and that another residue Thr415 plays an important role in assisting the maturation process. The activated Thr399 OG atom may directly attack the carbonyl group of Glu398 to form a transient tetrahedral intermediate, which is stabilized by the carbonyl of Glu419. The side chain of Glu419 is then held in its spatial position by the hydrogen bond networks involving Glu438, Asp441, Asn450, and a magnesium ion (Fig. 2A). In this respect, residue Asn450 may play a role in the autocatalytic processing of *Bl*GGT.

The catalytic site of *Bl*GGT has been identified by solving the crystal structure of its complex with L-glutamate [39]. The binding of L-glutamate occurs in a concave site lined by residues Arg109, Thr399, Glu438, Asp441, Ser460, Ser461, Gly481, and Gly482. As shown in Fig. 2B, Asn450 interacts with Asp441 by a hydrogen bond and consequently binds with Arg109 and Glu438 through the hydrogen bond network to hold the substrate in the proper position, suggesting that this residue can be also important for the catalytic function of *Bl*GGT.

3.2. Purification and biochemical characterization of wild-type and mutant enzymes

To evaluate the role of Asn450 in *Bl*GGT, this residue was replaced by four other amino acids through site-directed mutagenesis. Following expression and nickel-chelating affinity chromatography, protein samples were subjected to SDS – PAGE (Fig. 3A). The percentage of processing for each sample was then evaluated by measuring the intensity of the protein bands in the gels as described previously [35]. The experimental results indi-

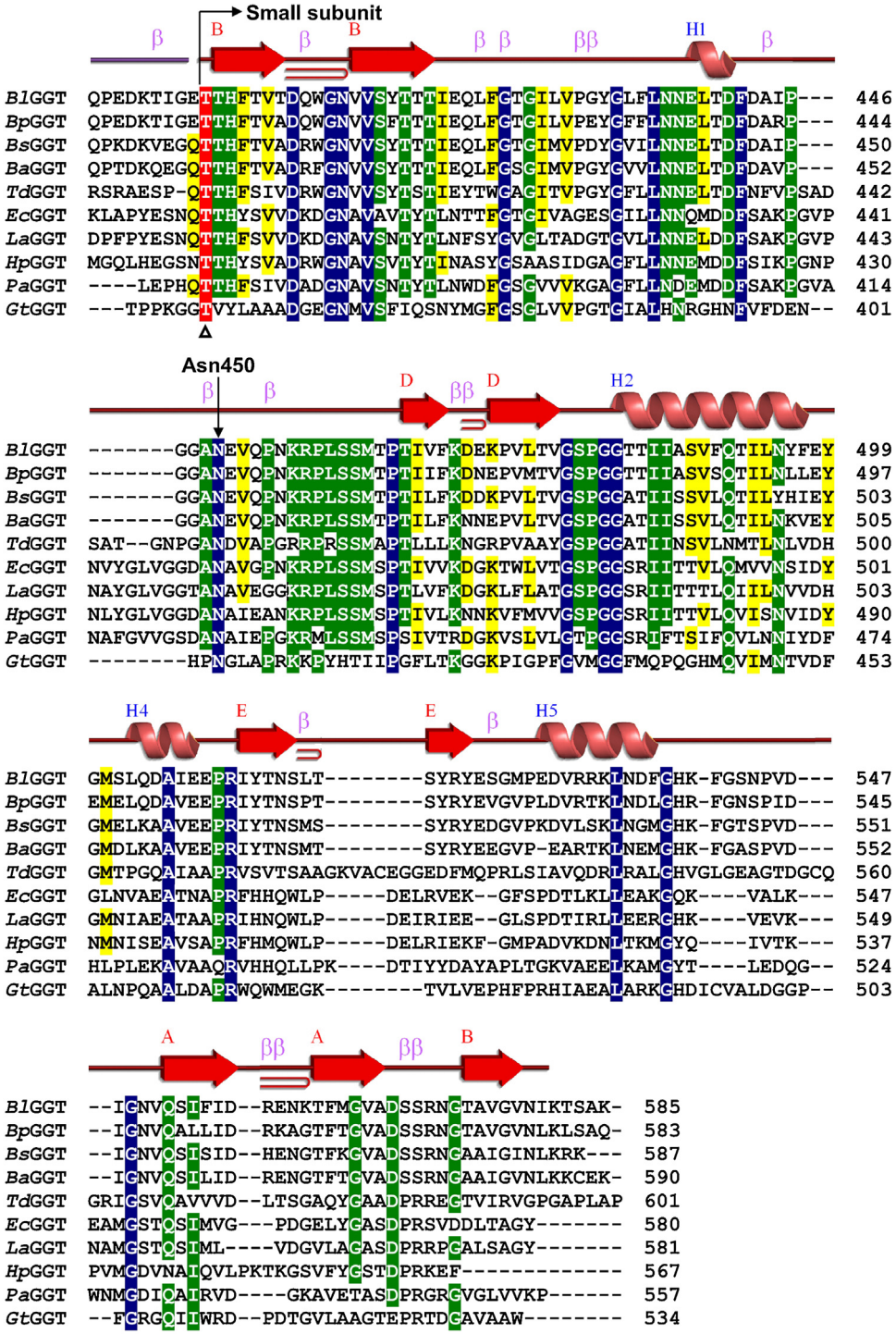

Fig. 1. Partial sequence alignment of *Bl*GGT and other bacterial counterparts. Three levels of conserved residues are shaded in blue (100%), green (80%) and yellow (60%), respectively. The putative active residue (Thr399) is marked by an open triangle. The secondary structure elements β-strands and α-helices are depicted as arrows and cylinders, respectively, above the sequence. The conserved Asn450 of *Bl*GGT is also indicated. (For interpretation of the references to color in this figure legend, the reader is referred to the web version of this article.)

cated that the freshly prepared *Bl*GGT had a percentage processing of 87.7 and, as compared with the wild-type enzyme, N450D was slightly improved in the self-processing of its precursor protein into a large and a small subunit. However, the percentage processing of N450Q, N450A, and N450 K was reduced to 63.6, 83.3, and 52.7%, respectively. Besides, all of N450 mutant proteins were able to autoprocess themselves into 41-kDa and 22-kDa subunits within 10 days (Fig. 3A). To examine whether changes to the catalytic function occurred as a result of mutations, the GGT activity of freshly purified *Bl*GGT, N450Q, N450A, N450D, and N450 K was accordingly measured. As shown in Fig. 3B, the wild-type enzyme had a transpeptidation activity of 11.41 ± 0.32 U/mg. N450 K only retained about 34.6% wild-type activity; conversely, a significant increase in the transpeptidation activity, with up to 3.6-fold enhancement, was observed in two versions of mutation. The specific transpeptidation activity of *Bl*GGT, N450Q, N450A, N450D,

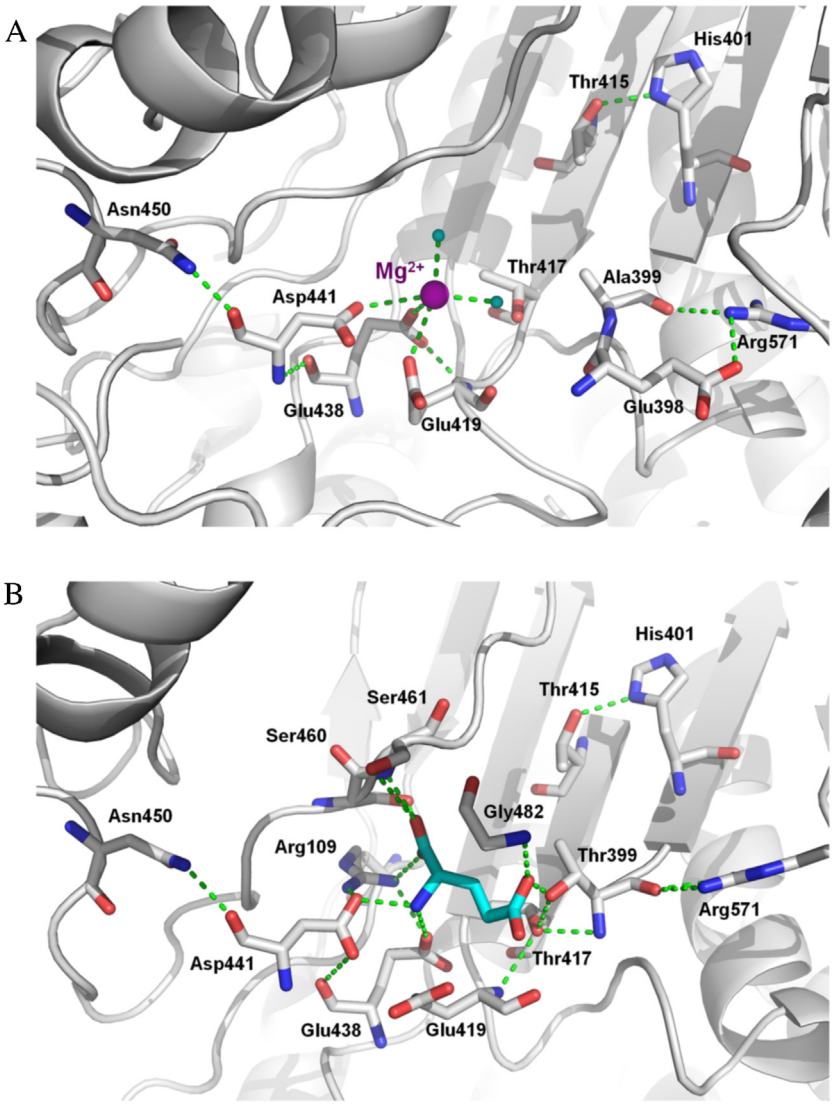

Fig. 2. Local environments surrounding the conserved Asn450 of *Bl*GGT. A) The autocatalytic environment of the T399A-*Bl*GGT structure (PDB code: 4Y23). B) L-Glu interactions in the active site of the *Bl*GGT structure (PDB code: 4OTT).

Table 2
Hydrolysis and transpeptidation activities of the mature enzymes.

Enzyme[a]	Specific activity (U/mg)[b]		Ratio (B/A)
	Hydrolysis (A)	Transpeptidation (B)	
*Bl*GGT	3.79 ± 0.31	13.31 ± 0.53	3.5
N450Q	1.66 ± 0.17	18.78 ± 0.68	11.3
N450A	2.91 ± 0.23	52.29 ± 2.69	18.0
N450D	3.61 ± 0.13	62.61 ± 4.59	17.4
N450K	1.27 ± 0.06	9.62 ± 1.31	7.6

[a] The purified enzymes were incubated at 4 °C for 10 days before activity assays.
[b] The specific activity was determined under the standard assay conditions in the absence (hydrolysis) and presence (transpeptidation) of Gly-Gly.

and N450 K was individually increased to 13.31 ± 0.53, 18.78 ± 0.68, 52.29 ± 2.69, 62.61 ± 4.59, and 9.62 ± 1.29 U/mg upon incubation of the enzyme samples at 4 °C for 10 days (Table 2). It is noteworthy that the ratio of transpeptidation to hydrolysis for the mature variants was increased from 3.5 to more than 7.6, in comparison with that of wild-type enzyme. The shift of catalytic behavior towards transpeptidation will provide some sort of positive benefits to the enzymatic synthesis of γ-glutamyl compounds. γ-Glutamyl derivatives are naturally occurring flavor enhancers found in many foods including cheese [50], mushrooms [51] and seasoning plants [52–54]. The potential applications of GGT enzymes in the biocatalytic synthesis of γ-glutamyl derivatives is sometimes suggested by analytical results, and, to date, only a few examples from the genus *Bacillus* are experimentally demonstrated at a preparative scale [55,56]. As *Bl*GGT exhibits transpeptidase activity towards some acceptor amino acids [26], its potential use as a biocatalyst for the biocatalytic synthesis of γ-glutamyl derivatives has been evaluated [57]. With the promising results from this study, a further step to employ N450A and N450D as the biocatalyst for the production of naturally occurring γ-glutamyl derivatives becomes significantly effective.

The K_M and k_{cat} values for *Bl*GGT were calculated to be 0.42 ± 0.02 mM and 16.04 ± 1.27 s^{-1}, respectively. It is worth to note that the kinetic parameters of N450Q were close to those of *Bl*GGT. As compared with the wild-type enzyme, N450 K exhibited 81% increase in K_M and 44.3% decrease in k_{cat}, leading to a profound reduction in its catalytic efficiency (Table 3). Besides, the catalytic efficiency of N450A and N450D mutants was dramatically increased by more than 3.7-fold. These results clearly indicate that single residue replacements at position 450 do not abolish the enzymatic activity but significantly change the cat-

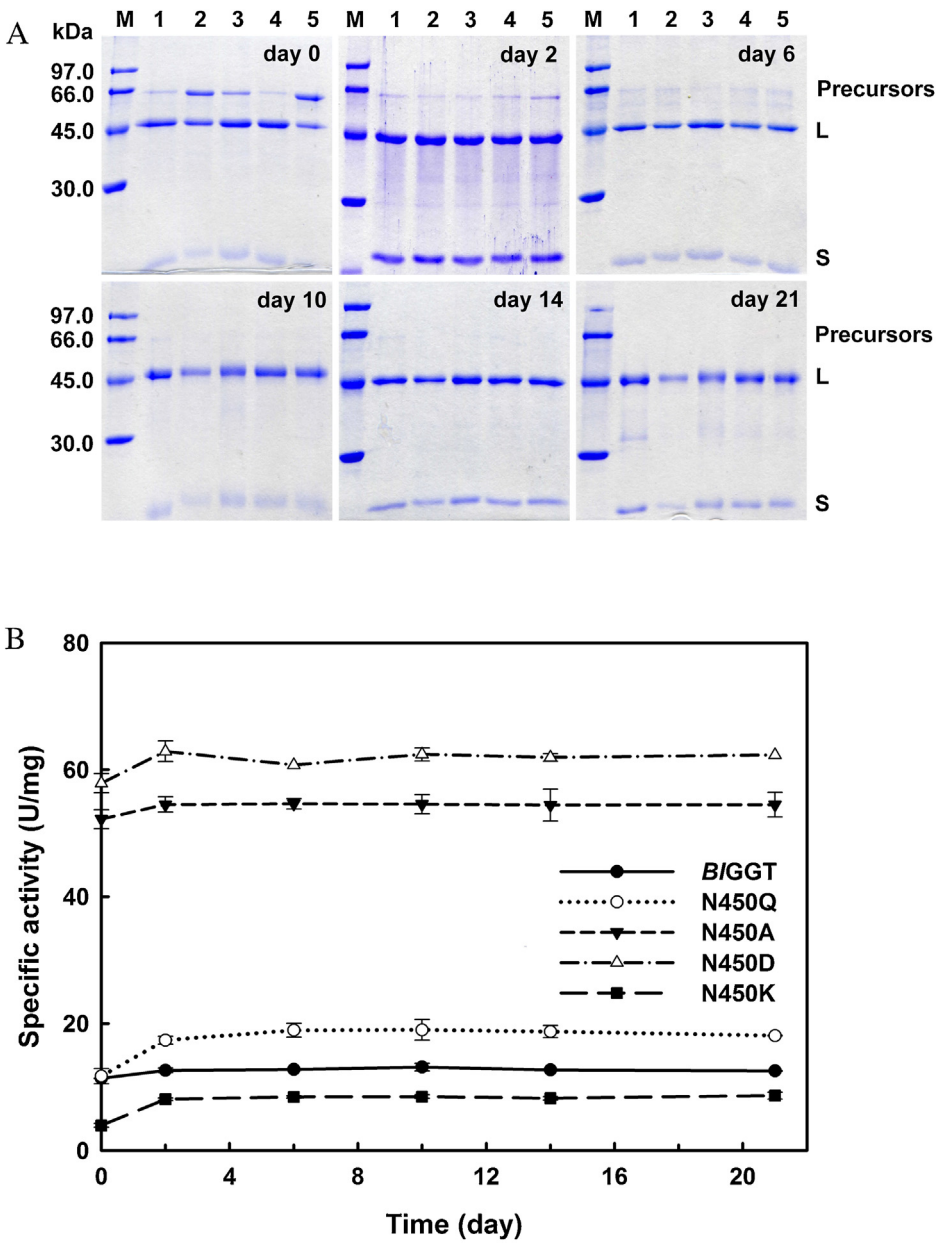

Fig. 3. Autocatalytic processing and generation of active form of *Bl*GGT and its variants. (A) SDS – PAGE analysis. Lanes: M, protein size markers; 1, *Bl*GGT; 2, N450Q; 3, N450A; 4, N450D; 5, N450 K. (B) The specific transpeptidation activity of purified enzymes as a function of time. Each point represents the mean of three independent determinations.

Table 3
Kinetic parameters of the mature enzymes.

Enzyme[a]	K_M (mM)	k_{cat} (s^{-1})	k_{cat}/K_M ($mM^{-1}\,s^{-1}$)
*Bl*GGT	0.42 ± 0.02	16.04 ± 1.27	38.19
N450Q	0.58 ± 0.03	21.74 ± 2.02	37.48
N450A	0.69 ± 0.05	123.65 ± 9.76	179.21
N450D	0.58 ± 0.02	175.52 ± 7.21	302.62
N450 K	0.76 ± 0.04	8.93 ± 0.09	11.75

[a] The purified enzymes were incubated at 4 °C for 10 days before kinetic assay.

alytic efficiency of *Bl*GGT. Due to the transpeptidase activity of *Bl*GGT is obviously affected by the mutations, it will be interesting to evaluate the steady-state kinetic parameters of wild-type and mutant enzymes with different donors/acceptor substrates in future. Relevant results may give us some insight into their catalytic mechanisms.

3.3. Spectroscopic analysis of wild-type and mutant enzymes

To evaluate possible structural changes that may result from single-point mutations, the protein conformation of wild-type *Bl*GGT and its mutant forms was analyzed using fluorescence and CD spectrometry. Fig. 4 shows the intrinsic fluorescence spectra of wild-type and mutant enzymes. As compared to the wild-type enzyme, the fluorescence intensity of N450Q, N450A, N450D, and N450 K was decreased by 3.8–43.5%. Alteration in fluorescence emission maxima was also noticeable. The tryptophan emission fluorescence spectrum for *Bl*GGT was maximized at a wavelength of 343.1 nm (Fig. 4). The λ_{max} of N450D, N450Q, and N450A individually exhibited 0.2, 0.6, and 1.8 nm red shift, and that of N450 K had a blue shift of 0.6 nm. These results suggest that minor structural changes have been occurred as a consequence of mutations. Conversely, the absence of major differences in the CD spectra of the wild-type and mutant enzymes indicated that the mutations

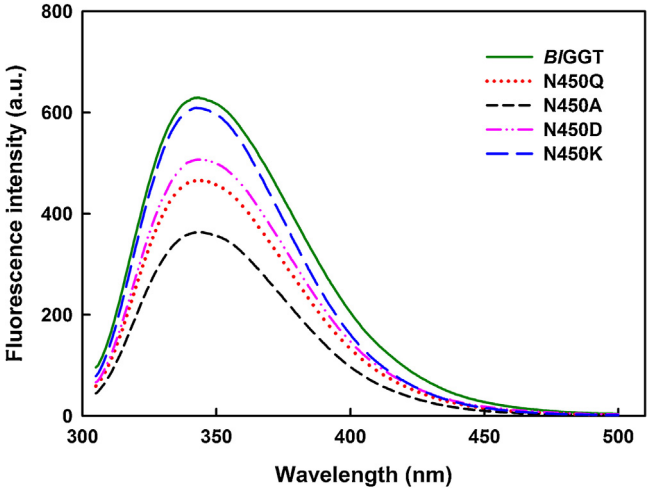

Fig. 4. Intrinsic fluorescence spectra of wild-type and mutant enzymes. An average of five spectra for each protein sample was recorded.

have no effect on the secondary structure of *Bl*GGT (Fig. 5A). Therefore, based on the criteria used in this study, we may discard a gross structural change as the explanation for the altered activity of the mutant enzymes.

The thermal denaturation of *Bl*GGT and *Ec*GGT has been shown to follow a two-state process [58], but that of the mature *Gt*GGT occurs through a three-state model [59]. In order to probe the conformation changes upon mutations of *Bl*GGT, temperature-induced denaturation of the secondary structure of wild-type and mutant enzymes was monitored by following the loss of ellipticity of the CD signal at 222 nm. As shown in Fig. 5B, temperature-dependent CD signals in the far-UV region displayed sigmoidal curves. *Bl*GGT began to unfold at around 54.2 °C and was completely unfolded at 69.3 °C; however, protein unfolding of the mutants started at 53.1 °C and ended around 67.4 °C. The transition curves clearly showed one transition with the apparent T_m values of 63.6 ± 0.5, 61.5 ± 1.4, 61.3 ± 0.3, 62.1 ± 0.3, and 59.3 ± 0.48 °C for *Bl*GGT, N450Q, N450A, N450D, and N450 K, respectively. Conclusively, the temperature-induced denaturation curves of wild-type and mutant enzymes are similar, implying that no dramatic changes in the secondary structure occurred as a result of Asn450 mutations.

Fluorescence spectra provide a sensitive means of characterizing proteins and their conformation. The fluorescence spectra of proteins are determined chiefly by the polarity of the environment of the tryptophan and tyrosine residues and by any specific interactions with nearby side chains [60]. In this regard, AEW that reports on the changes in both fluorescence wavelength and intensity was used to monitor the conformational stability of *Bl*GGT and its mutants. For *Bl*GGT, the AEW values in the absence of GdnHCl and at GdnHCl concentrations above 4.5 M were 343.2 and 357.1 nm, respectively. The unfolding transition was occurred at 3.6 M GdnHCl and a plateau region existed from 4.5 to 6.0 M (Fig. 6). Upon the treatment of *Bl*GGT with 6.0 M GdnHCl, the tryptophan emission λ_{max} of 348.5 nm could be seen. A fully exposed tryptophan in the unfolded protein shows emission λ_{max} approaching to 356 nm [60]. In this regard, the incubation of *Bl*GGT with higher concentrations of GdnHCl leads to the unfolding of the protein molecule. It is noteworthy that the $[GdnHCl]_{0.5,N\text{-}U}$ value for N450Q, N450A, N450D, and N450 K was reduced to 1.7, 2.1, 2.1, and 1.9 M, respectively. This result indicates that the structural stability of *Bl*GGT has been markedly altered by single residue replacements at position 450.

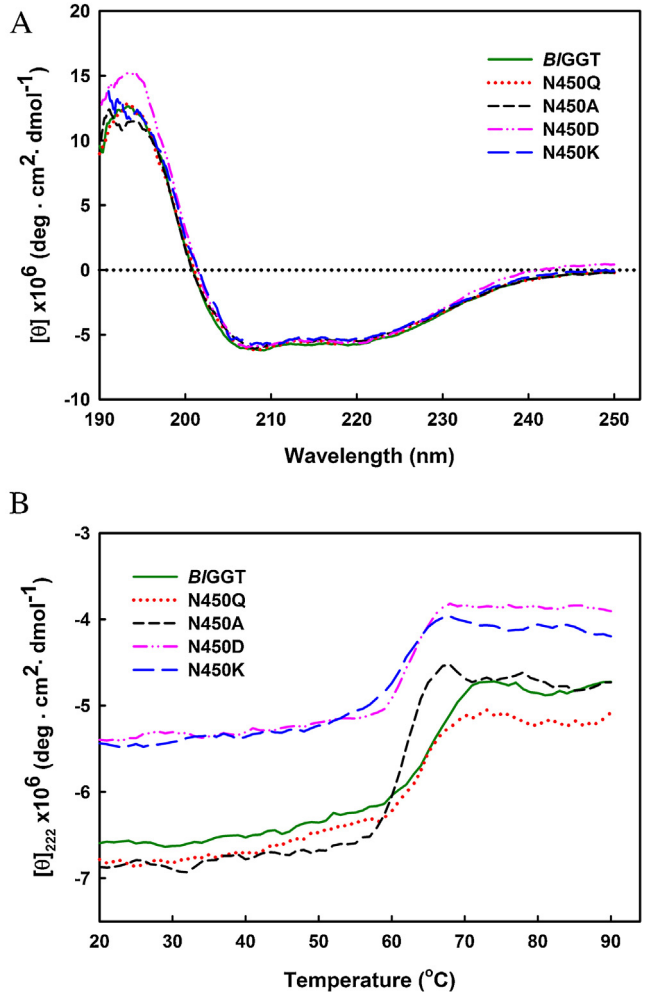

Fig. 5. CD analyses of wild-type and mutant enzymes. (A) Far-UV spectra of *Bl*GGT and its variants. The data were recorded at 22 °C and residual molar elliticities of the protein samples in 25 mM Tris-HCl buffer (pH 9.0) were measured from 190 to 250 nm. (B) Temperature-induced denaturation of *Bl*GGT and its variants. The protein samples in 25 mM Tris-HCl buffer (pH 9.0) were monitored with the CD signal at 222 nm.

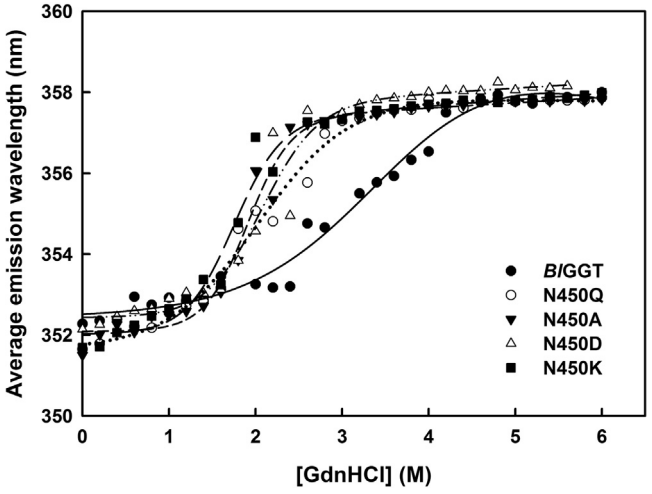

Fig. 6. GdnHCl-induced denaturation of *Bl*GGT and its variants. Data are presented as average emission wavelength, taking the value observed for native protein in the absence of GdnHCl as the control.

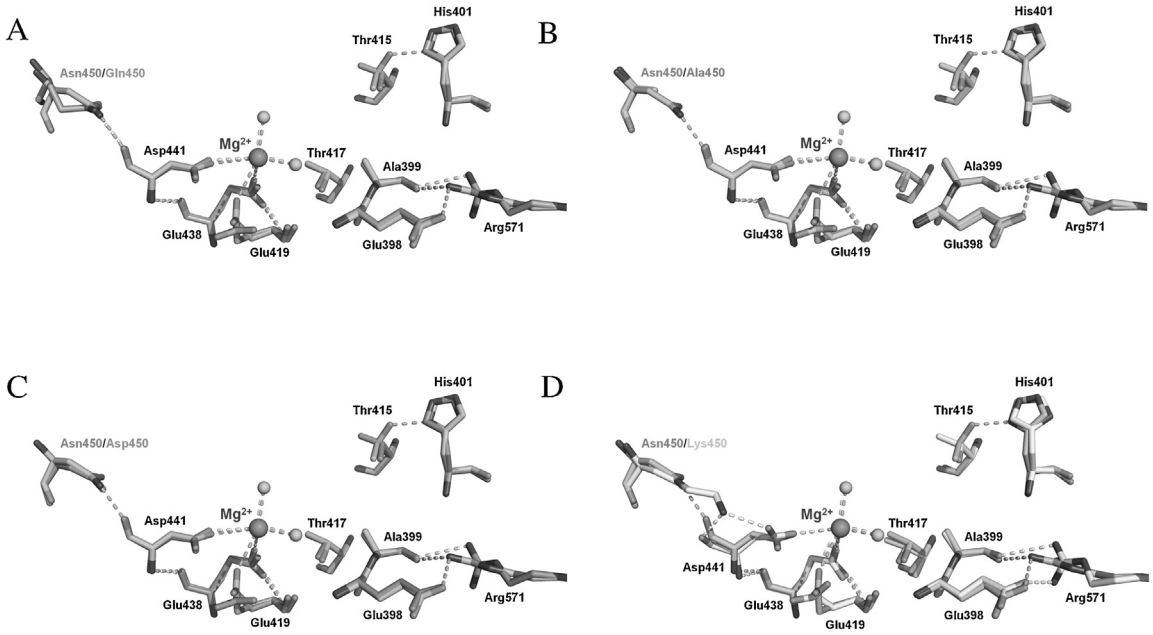

Fig. 7. Superimposition of the autocatalytic environment of wild-type and mutant enzymes. The autocatalytic environments were plotted by the program PyMOL. Residues Glu398, Ala399, His401, Thr415, Thr417, Glu419, Glu438, Asp441, and Arg571 are shown. The superimposition of wild-type enzyme with each variant was individually presented in panels A (N450Q), B (N450A), C (N450D), and D (N450 K).

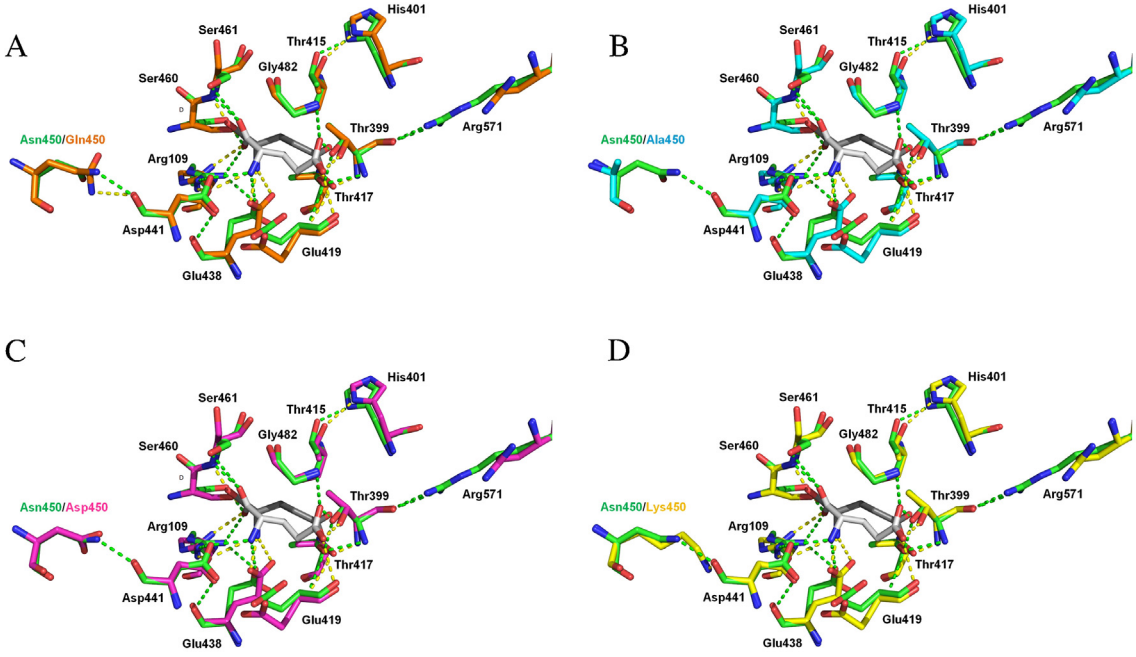

Fig. 8. Superimposition of the catalytic environment of wild-type and mutant enzymes. The catalytic environments were plotted by the program PyMOL. Residues Glu398, Ala399, His401, Thr415, Thr417, Glu419, Glu438, Asp441, and Arg571 are shown. The superimposition of wild-type enzyme with each variant was individually presented in panels A (N450Q), B (N450A), C (N450D), and D (N450K).

3.4. The impact of mutations on the local environment surrounding Asn450

To elucidate the mutational impact on *Bl*GGT, computer modeling of the local environments of Asn450 was performed on the basis of the X-ray crystal structures of *Bl*GGT (PDB code: 4OTT) and T399A-*Bl*GGT (PDB code: 4Y23) using Swiss Model Server. As aforementioned, residues Thr417 and Glu419 play an important role in the autocatalytic processing of *Bl*GGT. In the models of N450Q, N450A, and N450D (Fig. 7), it is apparently that the spatial arrangements of Thr417 and Glu419 are only slightly shifted from the original location of *Bl*GGT to new positions. However, a more profound shift in the spatial position of Thr417 is observed in N450 K. This may be the reason why the percentage processing of this variant goes down to 55.2%. In addition, the mutations also result in a position shift of Ala399 and Glu398 (Fig. 7). A previous study has been demonstrated that the distances between Gln390 O and Thr391 HG1 and Gln390C and Thr391 OG1 of *Ec*GGT are 2.05 and 2.56 Å, respectively, and the changes in distance between these two residues might affect the protonation of the carbonyl

oxygen atom of Gln390 and the formation of the oxyanion atom of Thr391 OG1 and may subsequently impair the autoprocessing ability of the enzyme [61]. Similarly, any change in the relative distance between the corresponding residues Thr399 and Glu398 may cause a drawback influence on the autocatalytic processing of *Bl*GGT.

Crystal structures of *Bl*GGT in the absence and presence of L-glutamate have already been solved [39]. According to those reported structures, Asn450 resides far away from the active site of *Bl*GGT and the effect of this residue on the catalytic activity of the enzyme is intriguing. However, it has been proposed that residues Arg109, Thr399, Glu438, Asp441, Ser460, Ser461, Gly481, and Gly482 are involved in the binding of the substrate [39]. As shown in Fig. 8, the model of N450Q displays a minimal alteration in the arrangement of these substrate-binding residues, so this is probably the reason that the catalytic activity of this variant was observed to be very similar to the wild-type enzyme. However, the active-site arrangement was notably changed upon the replacement of Asn450 with alanine, aspartic acid or lysine. The changes in the active-site conformation may be responsible for either the decrease or increase in the catalytic activity of *Bl*GGT.

4. Conclusion

The results of site-directed mutagenesis allow us to conclude that residue Asn450 is important for the catalytic function of *Bl*GGT. The replacements at position 450 of the enzyme lead to a slight reduction of the protein stability as revealed by the chemical-induced denaturation experiment. However, it is interesting that N450A and N450D showed both an enhanced activity towards the chromogenic substrate and an improved ratio of transpeptidation to hydrolysis. These two characteristics make them useful in the biocatalytic synthesis of γ-glutamyl derivatives. Molecular models of the mutant enzymes suggest that Asn450 might play a role in the maintenance of necessary environment for the maturation of precursor enzyme and might also relate to the proper binding of the substrate. However, future studies are needed to more precisely elucidate its structural roles, especially the determination of three-dimensional structures of N450A and N450D.

Conflict of interest

The authors have declared that there are no conflicts of interest.

Acknowledgements

The authors were eternally grateful for the research grant (MOST 103-2313-B-008-MY3) from Ministry of Science and Technology of Taiwan. The funder had no role in experimental design, data analysis and interpretation, decision to publish, and preparation of the manuscript.

References

[1] S. Tate, A. Meister, γ-Glutamyl transpeptidase: catalytic: structural and functional aspects, Mol. Cell. Biochem. 39 (1981) 357–368.
[2] N. Chikhi, N. Holic, G. Guellaen, Y. Laperche, γ-Glutamyltranspeptidase gene organization and expression: a comparative analysis in rat mouse, pig and human species, Comp. Biochem. Physiol. B Biochem. Mol. Biol. 122 (1999) 367–380.
[3] C. Jaspers, M. Penniuckx, Glutathione metabolism in *Saccharomyces cerevisiae*: evidence that γ-glutamyltranspeptidase is a vacuolar enzyme, Biochimie 66 (1984) 71–74.
[4] H. Suzuki, W. Hashimoto, H. Kumagai, Glutathione metabolism in *Escherichia coli*, J. Mol. Catal. B: Enzym. 6 (1999) 175–184.
[5] M. Hultberg, B. Hultberg, Glutathione turnover in human cell lines in the presence of agents with glutathione influencing potential with or with-out acivicin inhibition of γ-glutamyltranspeptidase, Biochim. Biophys. Acta 1726 (2005) 42–47.
[6] D.H. Lee, R. Blomhoff, D.R. Jacobs Jr., Is serum γ-glutamyltransferase a marker of oxidative stress? Free Radic. Res. 38 (2004) 535–539.
[7] R. Franco, J.A. Cidlowski, Apoptosis and glutathione: beyond an antioxidant, Cell Death Differ. 16 (2009) 1303–1314.
[8] A. Pompella, A. Corti, A. Paolicchi, C. Giommarelli, F. Zunino, γ-Glutamyltrnaspeptidase, redox regulation and cancer drug resistance, Curr. Opin. Pharmacol. 7 (2007) 360–366.
[9] D.H. Lee, D.R. Jacobs Jr., M. Gross, C.I. Kiefe, J. Roseman, C.E. Lewis, M. Steffes, γ-Glutamyltransferase is a predictor of incident diabetes and hypertension: the coronary artery risk development in young adults (CARDIA) study, Clin. Chem. 49 (2003) 1358–1366.
[10] D.H. Lee, M.H. Ha, J.H. Kim, D.C. Christiani, M.D. Gross, M. Steffes, R. Blomhoff, D.R. Jacobs Jr., γ-Glutamyltransferase and diabetes—a 4 year follow-up study, Diabetologia 46 (2003) 359–364.
[11] M.G. Betro, R.C. Oon, J.B. Edwards, γ-Glutamyltranspeptidase in diseases of the liver and bone, Am. J. Clin. Pathol. 60 (1973) 672–678.
[12] M. Emdin, C. Passino, M. Franzini, A. Paolicchi, A. Pompella, γ-Glutamyltransferase and pathogenesis of cardiovascular disease, Future Cardiol. 3 (2007) 263–270.
[13] S. Ahmad, L. Okine, R. Wood, J. Aljlan, D.T. Vistica, γ-Glutamyltranspeptidase (γ-GT) and maintenance of thiol pools in tumor cells resistant to alkylating agents, J. Cell. Physiol. 131 (1987) 240–246.
[14] L. Bouman, J. Sanceau, D. Rouillard, B. Bauvois, γ-Glutamyltranspeptidase expression in Ewing's sarcoma cells: up-regulation by interferons, Biochem. J. 364 (2002) 719–724.
[15] M.H. Hanigan, γ-Glutamyltranspeptidase: a glutathionase: its expression and function in carcinogenesis, Chem. Biol. Interact. 111–112 (1998) 333–342.
[16] A. Corti, M. Franzini, A. Paolicchi, A. Pompella, γ-Glutamyltransferase of cancer cells at the crossroads of tumor progression, drug resistance and drug targeting, Anticancer Res. 30 (2010) 1169–1181.
[17] H. Suzuki, C. Yamada, K. Kato, γ-Glutamyl compounds and their enzymatic production using bacterial γ-glutamyltranspetidase, Amino Acids 32 (2007) 333–340.
[18] I. Castellano, A. Merlino, γ-Glutamyltranspeptidases: sequence structure, biochemical properties, and biotechnological applications, Cell. Mol. Life Sci. 69 (2012) 3381–3394.
[19] W. Mu, T. Zhang, B. Jiang, An overview of biological production of L-theanine, Biotechnol. Adv. 33 (2015) 335–342.
[20] T. Okada, H. Suzuki, K. Wada, H. Kumagai, K. Fukuyama, Crystal structures of γ-glutamyltranspeptidase from *Escherichia coli* a key enzyme in glutathione metabolism, and its reaction intermediate, Proc. Natl. Acad. Sci. U.S.A. 103 (2006) 6471–6476.
[21] J.W. Keillor, R. Castonguay, C. Lherbet, γ-Glutamyltranspeptidase substrate specificity and catalytic mechanism, J. Phys. Org. Chem. 17 (2004) 529–536.
[22] J.W. Keillor, R. Castonguay, C. Lherbet, Pre-steady-state kinetic studies of rat kidney γ-glutamyltranspeptidase confirm its ping-pong mechanism, Methods Enzymol. 401 (2005) 449–467.
[23] I. Castellano, A. Merlino, M. Rossi, F. La Cara, Biochemical and structural properties of γ-glutamyl transpeptidase from *Geobacillus thermodenitrificans*: an enzyme specialized in hydrolase activity, Biochimie 92 (2010) 464–474.
[24] J.B. Whitfield, γ-Glutamyltranspeptidase, Crit. Rev. Clin. Lab. Sci. 38 (2001) 263–355.
[25] H. Suzuki, H. Kumagai, T. Tochikura, γ-Glutamyltranspeptidase from *Escherichia coli* K-12: purification and properties, J. Bacteriol. 168 (1986) 1325–1331.
[26] L.L. Lin, P.R. Chou, Y.W. Hua, W.H. Hsu, Overexpression one-step purification, and biochemical characterization of a recombinant γ-glutamyltranspeptidase from *Bacillus licheniformis*, Appl. Microbiol. Biotechnol. 73 (2006) 103–112.
[27] I. Castellano, A. Di Salle, A. Merlino, M. Rossi, F. La Cara, Gene cloning and protein expression of γ-glutamyltranspeptidases from *Thermus thermophilus* and *Deinococcus radiodurans*: comparison of molecular and structural properties with mesophilic counterparts, Extremophiles 15 (2011) 259–270.
[28] N.A. Murty, E. Tiwary, R. Sharma, N. Nair, R. Gupta, γ-Glutamyl transpeptidase from *Bacillus pumilus* KS 12: decoupling autoprocessing from catalysis and molecular characterization of N-terminal region, Enzyme Microb. Technol. 50 (2012) 159–164.
[29] G. Boanca, A. Sand, J.J. Barycki, Uncoupling the enzymatic and autoprocessing activities of *Helicobacter pylori* γ-glutamyltranspeptidase, J. Biol. Chem. 281 (2006) 19029–19037.
[30] M.B. West, S. Wickham, L.M. Quinalty, R.E. Pavlovicz, C. Li, M.H. Hanigan, Autocatalytic cleavage of human γ-glutamyltranspeptidase is highly dependent on *N*-glycosylation at asparagine 95, J. Biol. Chem. 286 (2011) 28876–28888.
[31] M. Inoue, J. Hiratake, H. Suzuki, H. Kumagai, K. Sakata, Identification of catalytic nucleophile of *Escherichia coli* γ-glutamyltranspeptidase by γ-monofluorophosphono derivative of glutamic acid: N-terminal Thr-391 in small subunit is the nucleophile, Biochemistry 39 (2000) 7764–7771.
[32] R.C. Lyu, H.Y. Hu, L.Y. Kuo, H.F. Lo, P.L. Ong, H.P. Chang, L.L. Lin, Role of the conserved Thr399 and Thr417 residues of a recombinant *Bacillus licheniformis* γ-glutamyltranspeptidase as evaluated by mutational analysis, Curr. Microbiol. 59 (2009) 101–106.
[33] H.P. Chang, W.C. Liang, R.C. Lyu, M.C. Chi, Z.F. Wang, K.L. Su, H.C. Hung, L.L. Lin, Effects of C-terminal truncation on the autocatalytic processing of a recombinant γ-glutamyltranspeptidase from *Bacillus licheniformis*, Biochemistry-Moscow 75 (2010) 919–929.

[34] M.C. Chi, Y.Y. Chen, H.F. Lo, L.L. Lin, Experimental evidence for the involvement of amino acid residue Glu398 in the autocatalytic processing of *Bacillus licheniformis* γ-glutamyltranspeptidase, FEBS Open Biol. 2 (2012) 298–304.
[35] M.C. Chi, Y.H. Lo, Y.Y. Chen, L.L. Lin, A. Merlino, γ-Glutamyl transpeptidase architecture: effect of extra sequence deletion on autoprocessing, structure and stability of the protein from *Bacillus licheniformis*, Biochim. Biophys. Acta 1844 (2014) 2290–2297.
[36] T. Okada, H. Suzuki, K. Wada, H. Kumagai, K. Fukuyama, Crystal structure of the γ-glutamyltranspeptidase precursor protein from *Escherichia coli*: structural changes upon autocatalytic processing and implications for the maturation mechanism, J. Biol. Chem. 282 (2007) 2433–2439.
[37] C. Oinonen, J. Rouvinen, Structural comparison of Ntn-hydrolases, Protein Sci. 9 (2000) 2329–2337.
[38] M.B. West, Y. Chen, S. Wickham, A. Heroux, K. Cahill, M.H. Hanigan, B.H. Mooers, Novel insights into eukaryotic γ-glutamyltranspeptidase 1 from the crystal structure of the glutamate-bound human enzyme, J. Biol. Chem. 288 (2013) 31902–31913.
[39] L.L. Lin, Y.Y. Chen, M.C. Chi, A. Merlino, Low resolution X-ray structure of γ-glutamyltranspeptidase from *Bacillus licheniformis*: opened active site cleft and a cluster of acid residues potentially involved in the recognition of a metal ion, Biochim. Biophys. Acta 1844 (2014) 1523–1529.
[40] K. Wada, M. Irie, H. Suzuki, K. Fukuyama, Crystal structure of the halotolerant γ-glutamyltranspeptidase from *Bacillus subtilis* in complex with glutamate reveals a unique architecture of the solvent-exposed catalytic pocket, FEBS J. 277 (2010) 1000–1009.
[41] A. Pica, M.C. Chi, M. D'Ischia, Y.Y. Chen, L.L. Lin, A. Merlino, The maturation mechanism of γ-glutamyltranspeptidases: insights from the crystal structure of a precursor mimic of the enzyme from *Bacillus licheniformis*, Biochim. Biophys. Acta 1864 (2016) 195–203.
[42] M.A. Larkin, G. Blackshields, N.P. Brown, R. Chenna, P.A. McGettigan, H. McWilliam, F. Valentin, I.M. Wallace, A. Wilm, R. Lopez, J.D. Thompson, T.J. Gibson, D.G. Higgins, Clustal W and Clustal X version 2.0, Bioinformatics 23 (2007) 2947–2948.
[43] K. Arnold, L. Bordoli, J. Kopp, T. Schwede, The SWISS-MODEL Workspace: a web-based environment for protein structure homology modelling, Bioinformatics 22 (2006) 195–201.
[44] P. Emsley, K. Cowtan, Coot: model-building tools for molecular graphics, Acta Crystallogr. D60 (2004) 2126–2132.
[45] P.D. Adams, P.V. Afonine, G. Bunkoczi, V.B. Chen, I.W. Davis, N. Echols, J.J. Headd, L.W. Hung, G.J. Kapral, R.W. Grosse-Kunstleve, A.J. McCoy, N.W. Moriarty, R. Oeffner, R.J. Read, D.C. Richardson, J.S. Richardson, T.C. Terwilliger, P.H. Zwart, PHENIX: a comprehensive Python-based system for macromolecular structure solution, Acta Crystallogr. D66 (2010) 213–221.
[46] U.K. Laemmli, Cleavage of structural proteins during the assembly of the head of bacteriophage T4, Nature 227 (1970) 680–685.
[47] H.Y. Hu, J.C. Yang, J.H. Chen, M.C. Chi, L.L. Lin, Enzymatic characterization of *Bacillus licheniformis* γ-glutamyltranspeptidase fused with N-terminally truncated forms of *Bacillus* sp. TS-23 α-amylase, Enzyme Microb. Technol. 51 (2012) 86–94.
[48] T.K. Chaudhuri, M. Arai, T.P. Terada, T. Ikura, K. Kuwajima, Equilibrium and kinetic studies on folding of the authentic and recombinant forms of human α-lactalbumin by circular dichroism spectroscopy, Biochemistry 39 (2000) 15643–15651.
[49] H. Suzuki, H. Kumagai, Autocatalytic processing of γ-glutamyltranspeptidase, J. Biol. Chem. 277 (2002) 43536–43543.
[50] S. Toelstede, A. Dunkel, T. Hofmann, A series of kokumi peptides impart the long-lasting mouthfulness of matured gouda cheese, J. Agric. Food Chem. 57 (2009) 1440–1448.
[51] S. Hatanaka, Amino acids from mushrooms, Prog. Chem. Org. Nat. Prod. 59 (1992) 1–140.
[52] Y. Ueda, M. Sakaguchi, K. Hirayama, R. Miyajima, A. Kimizuka, Characteristic flavor constituents in water extract of garlic, Agric. Biol. Chem. 54 (1990) 163–169.
[53] H.A. Wetli, R. Brenneisen, I. Tschudi, M. Langos, P. Bigler, T. Sprang, S. Schuerch, R.C. Muehlbauer, A γ-glutamyl peptide isolated from onion (*Allium cepa* L.) by bioassay-guided fractionation inhibits resorption activity of osteoclasts, J. Agric. Food Chem. 53 (2005) 3408–3414.
[54] C. Starkenmann, Y. Niclass, I. Cayeux, Occurrence of L-γ-glutamyl-S-(1-hydroxy-2-methyl-3-pentanyl)-L-cysteine and S-(1-ethyl-3-hydroxy-2-methylpropyl)-L-cysteine in fresh and processed *Allium caepa* L. cultivar, Flav. Fragr. J. 26 (2011) 378–384.
[55] H. Suzuki, K. Kato, H. Kumagai, Development of an efficient enzymatic production of γ-D-glutamyl-L-tryptophan (SCV-07) a prospective medicine for tuberculosis, with bacterial γ-glutamyltranspeptidase, J. Biotechnol. 111 (2004) 291–295.
[56] Y. Shuai, T. Zhang, B. Jiang, W. Mu, Development of efficient enzymatic production of theanine by γ-glutamyltranspeptidase from a newly isolated strain of *Bacillus subtilis*, SK11.004, J. Sci. Food Agric. 90 (2010) 2563–2567.
[57] Y.Y. Chen, H.F. Lo, T.F. Wang, M.G. Lin, L.L. Lin, M.C. Chi, Enzymatic synthesis of γ-L-glutamyl-*S*-allyl-L-cysteine a naturally occurring organosulfur compound from garlic, by *Bacillus licheniformis* γ-glutamyltranspeptidase, Enzyme Microb. Technol. 75-76 (2015) 18–24.
[58] J.C. Yang, W.C. Liang, Y.Y. Chen, M.C. Chi, H.F. Lo, H.L. Chen, L.L. Lin, Biophysical characterization of *Bacillus licheniformis* and *Escherichia coli* γ-glutamyltranspeptidases: a comparative analysis, Int. J. Biol. Macromol. 48 (2011) 414–422.
[59] A. Pica, I.R. Krauss, I. Castellano, M. Rossi, F. La Cara, G. Graziano, F. Sica, A. Merlino, Exploring the unfolding mechanism of γ-glutamyltranspeptidases: the case of the thermophilic enzyme from *Geobacillus thermodenitrificans*, Biochim. Biophys. Acta 1824 (2012) 571–577.
[60] C.A. Royer, Probing protein folding and conformational transitions with fluorescence, Chem. Rev. 106 (2006) 1769–1784.
[61] P.L. Ong, Y.F. Yao, Y.M. Weng, W.H. Hsu, L.L. Lin, Residues Arg114 and Arg337 are critical for the proper function of *Escherichia coli* γ-glutamyltranspeptidase, Biochem. Biophys. Res. Commun. 366 (2008) 294–300.